NANOSIM

Laboratory for Simulations of Nanostructured Systems

http://phys.ubbcluj.ro/~tbeu/nanosim.html

Gene Delivery

- **Gene therapy** – remarkable potential to cure genetic or acquired diseases
- **Central mechanism – DNA condensation** into **polyplexes** capable of **transfection**
- **Genetic vectors** (gene carriers):
  - wrap / condensate / protect DNA
  - release DNA inside the cell
- **Polyethyleneimine** $[-CH_2-NH-CH_2-]_n$
  - large buffering capacity
  - simple engineering
- **DNA-PEI polyplexes** – ruled by electrostatics:
  - phosphate groups of DNA (–)
  - amino groups of PEI (+)
- **Main aim** – **investigate DNA-PEI condensation** required scale > 2 000 000 atoms

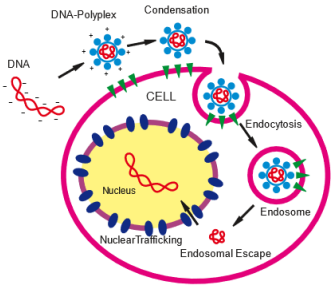

Gene transfer via non-viral vectors.
After Lungwitz et al. Biopharmaceutics 60 (2005) 247.

Modeling levels of PEI

- **Ab initio**
  - Quantum mechanical (QM) calculations on **PEI models**
  - ~25 Å, ~50 atoms
  - Gaussian 09
- **Atomistic (AA)**
  - **Development of a CHARMM FF for PEI**
  - Reference data: QM calculations
  - MD simulations of solvated PEI chains
  - Validation: experimental data
  - ~100 Å, ~100 000 atoms
  - ffTk 1.1
  - NAMD 2.13
- **Coarse-Grained (CG)**
  - **Development of a MARTINI FF for PEI**
  - Reference: AA simulations
  - MD simulations of solvated PEI chains and DNA-PEI polyplexes
  - Validation: AA and experimental data
  - ~250 Å, ~450 000 beads (equivalent to ~2 000 000 atoms)
  - Gromacs 2018.1
  - NAMD 2.13

The CHARMM Force Field

- **Atomistic force field** based on **atom** and **residue types**
- **Intramolecular (bonded) terms** – between atom types:

CHARMM parameters to be optimized

$$U_{\text{bonded}} = \sum_{\text{bonds}} k_b(b-b_0)^2 + \sum_{\text{angles}} k_\theta(\theta-\theta_0)^2 + \sum_{\text{dihedrals}} k_\psi[1+\cos(n\psi-\delta)]$$

- **Intermolecular (non-bonded) terms**:

$$U_{\text{non-bonded}} = \sum_{\text{atoms } i,j} \left\{ \frac{q_i q_j}{\epsilon_0 r_{ij}} + \varepsilon_{ij}\left[\left(\frac{r_{ij}^{\min}}{r_{ij}}\right)^{12} - 2\left(\frac{r_{ij}^{\min}}{r_{ij}}\right)^{6}\right]\right\}$$

$$r_{ij}^{\min} = (r_i^{\min} + r_j^{\min})/2, \qquad \varepsilon_{ij} = \sqrt{\varepsilon_i \varepsilon_j}$$

K. Vanommeslaeghe, ... A. D. MacKerell Jr., J. Comput. Chem., 2010, **31**, 671.

Atomistic CHARMM model for PEI

- **Reference QM properties**:
  ab initio calculations on **PEI models** Gaussia...
  MP2/6-31G(d)
- **Residue types**:
  - **PEI** – generic PEI monomer $–[CH_2–NH–CH_2]–$
  - **PEP** – protonated monomer $–[CH_2–NH_2^+–CH_2]–$
  - **PEC** – terminal CH_3 group
- **Atom types**:
  - NH1, HN1, CH2, HC2 (PEI)
  - NH2P, HN2P, CH2P (PEP)
  - CH3, HC3 (PEC)

PEI5p0 non-protonated

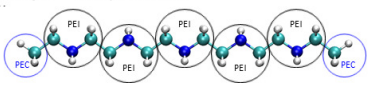

PEI5p1 central protonation

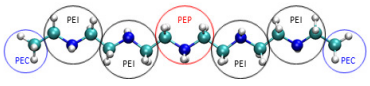

PEI5u2 uniform protonation

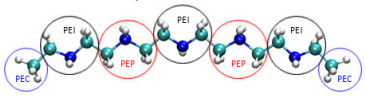

Beu, Farcaş, J. Comput. Chem. 38, 2335 (2017).
Beu, Ailenei, Farcaş, J. Comput. Chem. **39**, 2564 (2018).

MD simulations of solvated PEI

Reference Simulation Set:

- PEI 27-mer, 39-mer, 51-mer
- Protonation fractions: 0, 1/4, 1/3, 1/2

NPT simulations ~70000 atoms
PME (Particle-Mesh-Ewald) electrostatics
400 ns data collection (time step 2 fs)

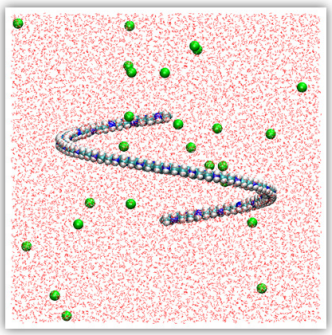

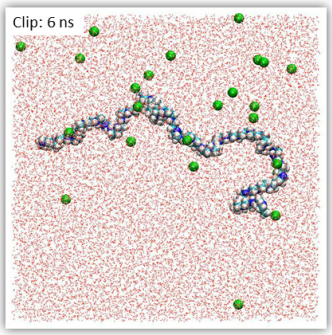

The MARTINI Force Field

- **Coarse-grained force field** based on **bead types**
- **Intramolecular (bonded) terms** – between bead types:

MARTINI parameters to be optimized

$$U_{\text{bonded}} = \frac{1}{2}\sum_{\text{bonds}} K_b(b-b_0)^2 + \frac{1}{2}\sum_{\text{angles}} K_\theta(\theta-\theta_0)^2 + \sum_{\text{dihedrals}} K_\psi[1+\cos(n\psi-\delta)]$$

- **Intermolecular (non-bonded) terms**:

$$U_{\text{non-bonded}} = \sum_{\text{beads } i,j}\left\{\frac{q_i q_j}{\epsilon_0 r_{ij}} + \varepsilon_{ij}\left[\left(\frac{r_{ij}^{\min}}{r_{ij}}\right)^{12} - 2\left(\frac{r_{ij}^{\min}}{r_{ij}}\right)^{6}\right]\right\}$$

J. Marrink, H. J. Risselada, ... and A. H. de Vries, J. Phys. Chem. B, **2007**, 111, 7812.

Coarse-grained MARTINI model for PEI

- **MARTINI force field**:
  - ~4 heavy atoms → **bead**
  - 10-fold reduction of objects
  - 10-fold increase of time step
- **Standard bead types** → vdW interactions: Q–charged, P–polar, N–nonpolar, C–apolar
  - **Q and N subtypes**: d–donor, a–acceptor, da–both, 0–none
  - **P and C:** 5 degrees of polarity
  - **Small "S"** and tiny "T" variants
  - Interaction levels (strengths): 10
- **Bead types tested for PEI**:
  - **PEI** – Nda, Nd, N0, SNda, SNd, SN0
  - **PEP** – Qda, Qd, Q0, SQda, SQd, SQ0
  - **PEC** – same as PEI

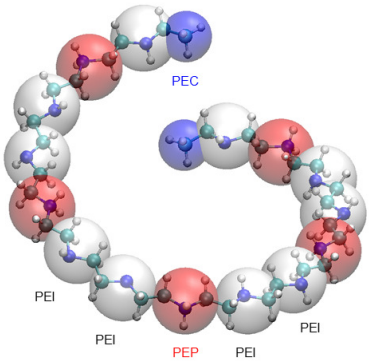

T. A. Beu, A. E. Ailenei, A. Farcaş, Chem. Phys. Lett. 714, 94-98 (2019).

MARTINI water

- **Standard water**:
  - W beads (P4-type) map 4 H2O mols
  - WF beads (BP4-type "big antifreeze") replace 1 in 10 Ws – to avoid freezing at to high temperatures
- **Polarizable water**:
  - (W, WM, WP) beads map 4 H2O mols
  - W-WM and W-WP distances constrained
  - W – only Lennard-Jones interactions
  - WM and WP – only Coulomb interactions

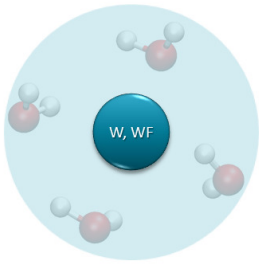

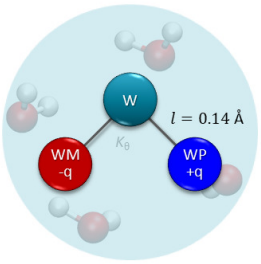

MARTINI Types and Non-Bonded Parameters

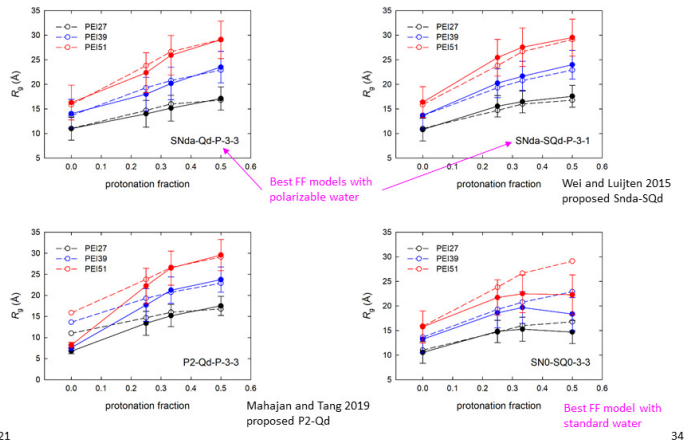

Structure of DNA

DNA – polymer composed of nucleotides
Nucleotides: nucleobase
sugar (deoxyribose)
phosphate group

A **Adenine** T **Thymine**

G **Guanine** C **Cytosine**

Purines

Pirimidines

Sugar phosphate backbone

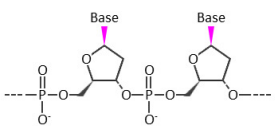

DNA strands held together by **H-bonds**

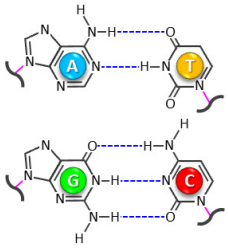

MARTINI model for DNA

J. J. Uusitalo,... S. J. Marrink, J. Chem. Theory Comput. 2015, 11, 3932.

- Nucleotides mapped to 6 or 7 beads
- **Backbone** – BB1, BB2, BB3
- **Adenine** – ASC1, ASC2, ASC3, ASC4

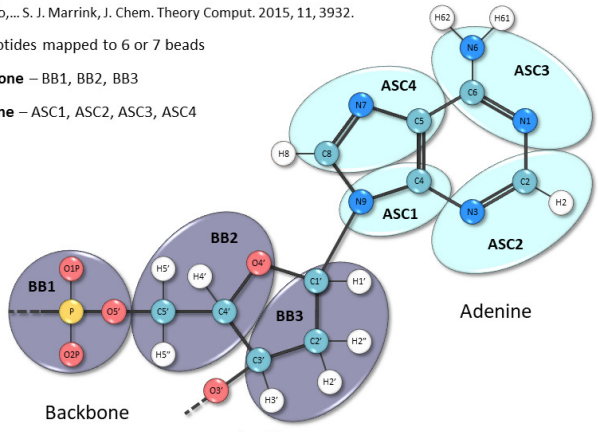

Drew-Dickerson DNA Dodecamer

AA CHARMM model

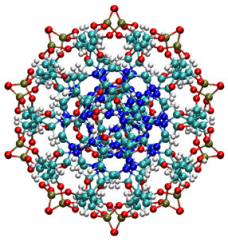

CGCGAATTCGCG
GCGCTTAAGCGC

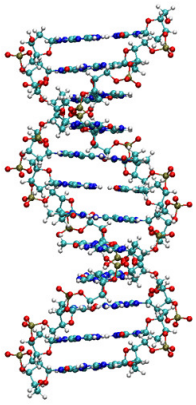

Drew-Dickerson DNA Dodecamer

CG MARTINI model
Home-made "martinization" code

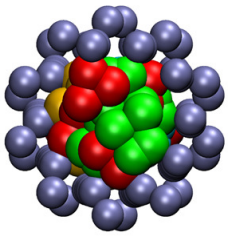

A Adenine T Thymine
G Guanine C Cytosine

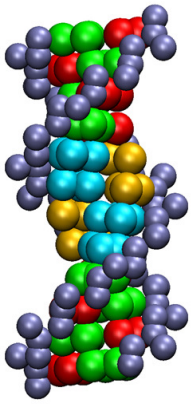

Formation of DNA-PEI complexes

2 Drew-Dickerson dodecamers + 4 PEI15 protonated 1/2
8100 beads (~32000 atoms) – 96% polarized water
Simulation box: 68 x 68 x 68 Å (PBC), time step 10 fs

Nucleobase
Backbone
PEI
Na

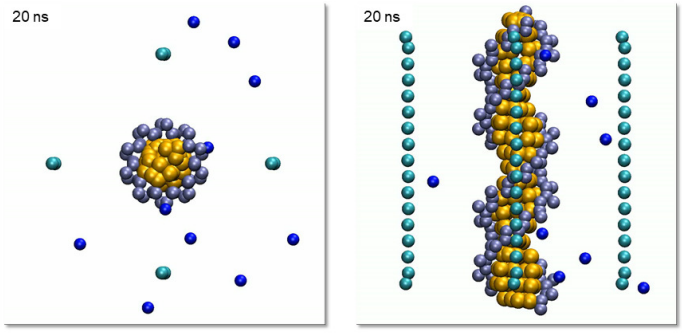

Condensation of DNA-PEI polyplexes

30 Drew-Dickerson dodecamers + 22 PEI 65-mers protonated 1/2
440 000 beads (~1 800 000 atoms) – 98% polarizable water
Simulation box (PBC): 260 x 260 x 260 Å, time step 10 fs

Nucleobase
Backbone
PEI
Na

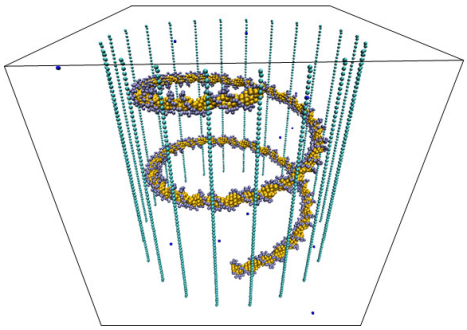

Condensation of DNA-PEI polyplexes

30 Drew-Dickerson dodecamers + 22 PEI 65-mers protonated 1/2
440 000 beads (~1 800 000 atoms) – 98% polarizable water
Simulation box (PBC): 260 x 260 x 260 Å, time step 10 fs

Nucleobase
Backbone
PEI

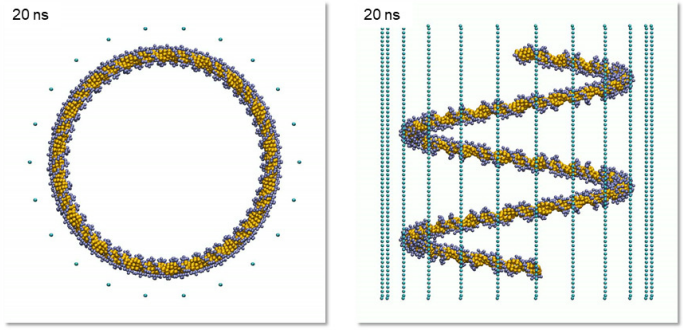

Radiation-induced fragmentation of fullerenes

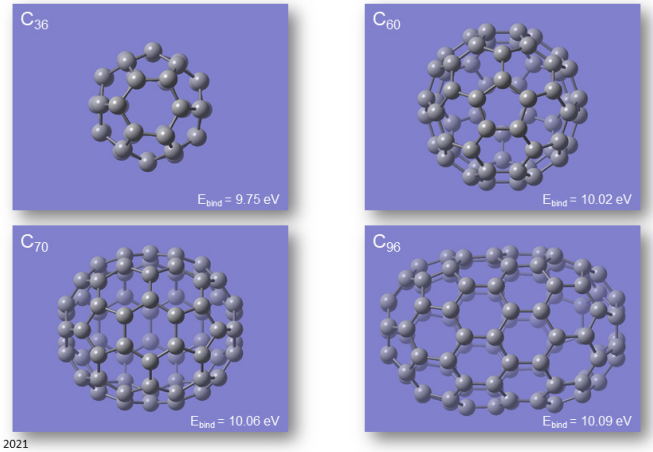

Radiation-induced fragmentation of fullerenes

C60
qtot = +10e, Eexc = 50 eV

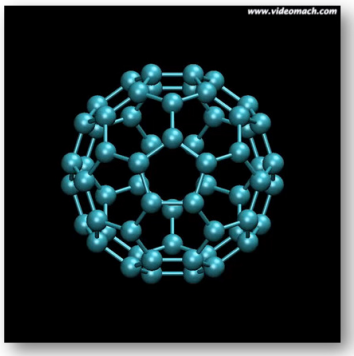

C60
qtot = +10e, Eexc = 100 eV

Radiation-induced fragmentation of fullerenes

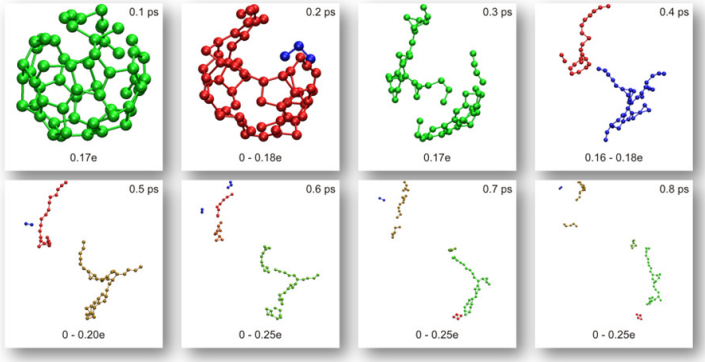

Radiation-induced fragmentation of fullerenes

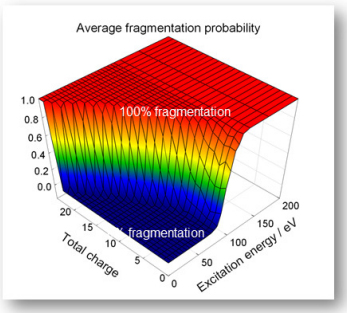

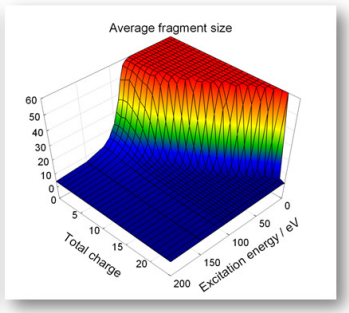

Fragmentation probability (for each parameter combination) – ratio of dissociative trajectories to total number of trajectories

Phase transition: fragmentation-less regime ($p = 0$) → saturation regime ($p = 1$)

Carbon nanotubes

1991 – Discovery of multi-wall CNTs – S. Iijima, Nature **354**, 56 (1991).

1993 – Synthesis of single-wall CNTs – S. Iijima & T. Ichihashi, Nature, **363**, 603 (1993).

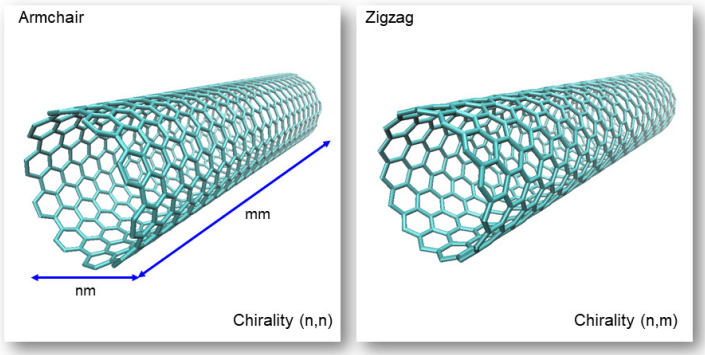

Carbon nanotubes

- **Extreme length-to-diameter ratio** up to 132,000,000:1
  a few nm in diameter, up to a mm long.
- **Exceptional material properties** – strength, stiffness, toughness, electrical and thermal conductivity etc.
- **Stiffness** (Young's modulus) up to 1000 GPa – 5x stiffer than steel.
- **Metallic or semiconducting character** depending on the CNT structure.
- **Gas flow** exceeds predictions of the Knudsen diffusion model by > 1 order.
- **Water flow** exceeds values from continuum hydrodynamics by > 3 orders.
- **Huge flow rates** of solvents ~ independent of pore length.
- **Quasi-frictionless transport**.
- **Wide variety of applications**: filtration, electronics, catalysis, molecular sensing etc.

Carbon nanotubes as mass resonators
CNT (6,6) 30 – breathing modes

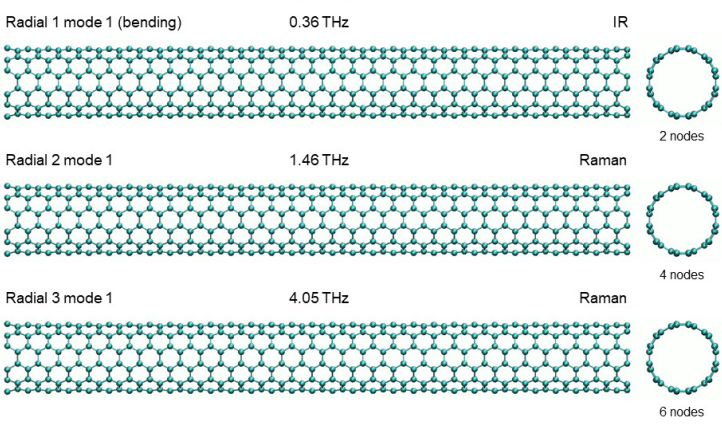

Carbon nanotubes as mass resonators
CNT (6,6) 30 – twisting, stretching, and scissoring

Twisting mode 1 1.00 THz Raman

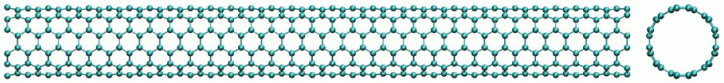

Stretching mode 1 1.53 THz Raman

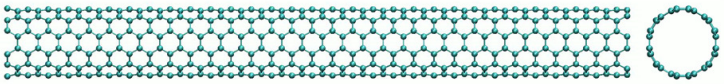

Scissoring mode 1 5.73 THz Raman

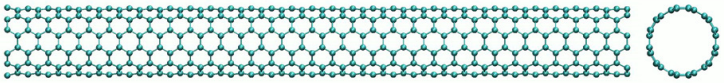

Carbon nanotubes as mass resonators
CNT (6,6) 30 – twisting, stretching, and scissoring

Twisting mode 2 2.01 THz Raman

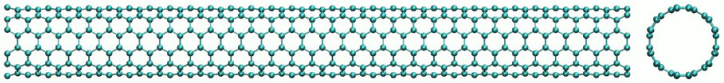

Stretching mode 2 3.06 THz Raman

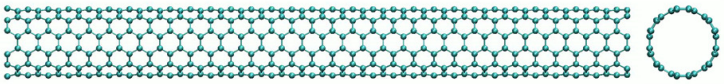

Scissoring mode 2 6.29 THz Raman

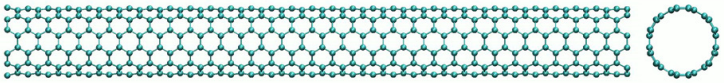

Frequency doubling for lowest twisting and stretching modes
Above 10 THz, stretching modes goes over into radial modes

Carbon nanotubes as mass resonators
Fundamental modes

Radial 1 (bending)

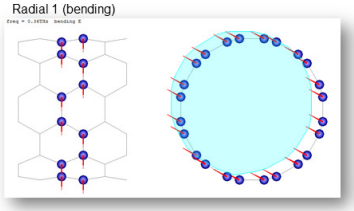

Radial 2

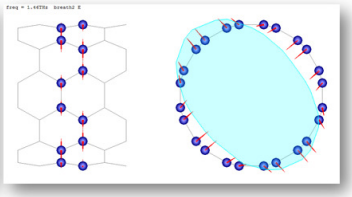

Radial 3

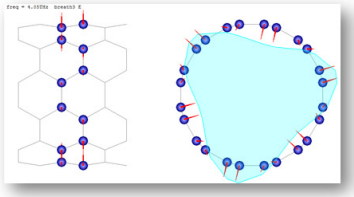

Radial 4

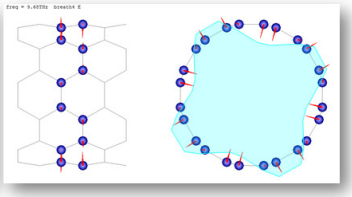

Carbon nanotubes as mass resonators
Fundamental modes

Axial 0 (stretching)

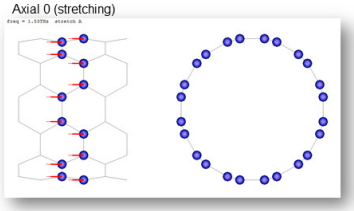

Radial 0 (breathing)

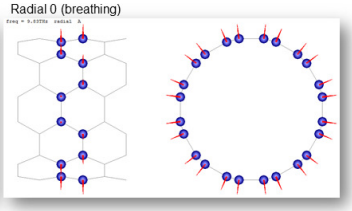

Axial 1 (scissoring)

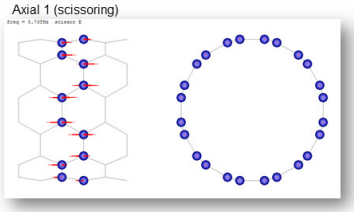

Twisting

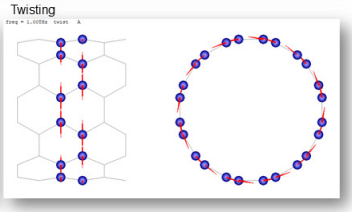

Carbon nanotubes as mass resonators
Merit functions

- **Twisting** – cumulated (axial) vector products of transversal displacements

$$F_t = \sum_{\Delta_z} \left| \sum_{i \in \Delta_z} (x_i \cdot \delta x_i - y_i \cdot \delta y_i) \right|$$

- **Radial Fourier analysis**

$$F_r^n = 1 - \sum_{\Delta_z} \sum_{i \in \Delta_z} \left| \cos n\varphi_i - \frac{\delta r_i}{\delta r_{\max}} \right|$$

- **Axial Fourier analysis**

$$F_z^n = 1 - \sum_{\Delta_z} \sum_{i \in \Delta_z} \left| \cos n\varphi_i - \frac{\delta z_i}{\delta z_{\max}} \right|$$

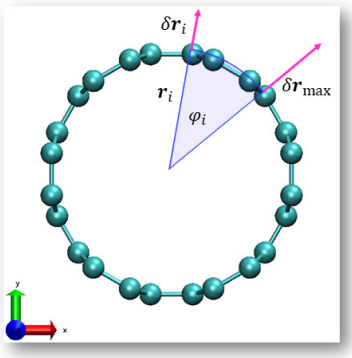

Carbon nanotubes as mass resonators
Length-dependence of normal frequencies for clamped-clamped CNTs

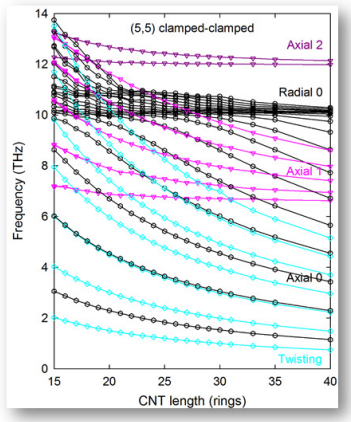

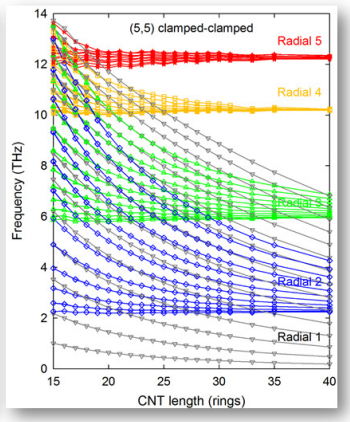

Carbon nanotubes for filtration/separation applications
CNT model

Chirality	r_{pore}	r_{pore}^{eff}	z_{pore}	z_{pore}^{eff}	x_{cell}	y_{cell}	z_{cell}	V_{pore}^{eff} / V_{fill}^{eff}	No. of C atoms
(8,8)	5.42	3.74	30.09	31.76	14.89	14.74	47.21	0.09	1368
(9,9)	6.09	4.42	30.09	31.76	14.89	14.74	46.58	0.13	1436
(10,10)	6.77	5.10	30.09	31.76	14.89	14.74	45.85	0.17	1522
(11,11)	7.45	5.77	30.09	31.76	14.89	14.74	45.01	0.22	1606
(12,12)	8.12	7.45	30.09	31.76	14.89	13.51	45.19	0.28	1630

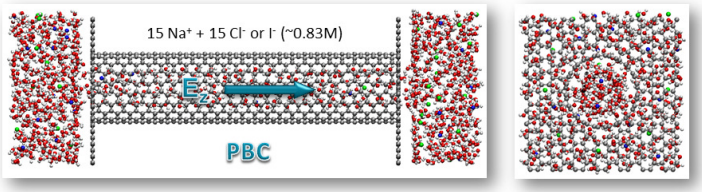

Carbon nanotubes for filtration/separation applications
Polarized pore charge distributions – "Charge-hopping" Monte Carlo method

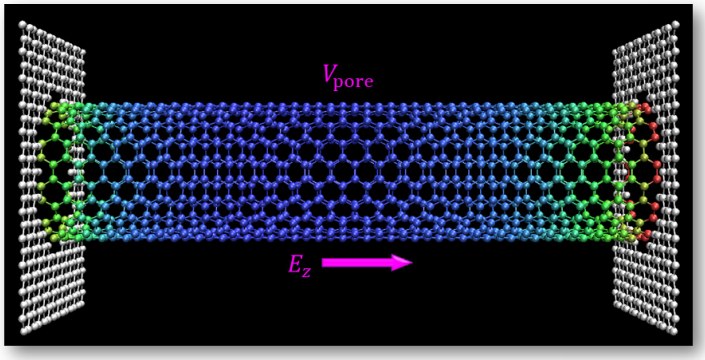

- Constrained minimum for the total Coulomb energy with fixed total charge / voltage
- **Interactions**: (1) between charges and electric fields, (2) between charges, (3) self-energies.
- Multiple Monte Carlo threads, averaged at the end.

Carbon nanotubes for filtration/separation applications
Typical run

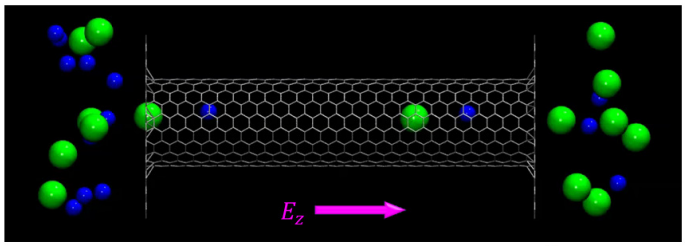

- Water molecules are not shown
- 6 ns of a trajectory are presented

Carbon nanotubes for filtration/separation applications
Solution structuring

Radial density profiles **Axial density profiles**

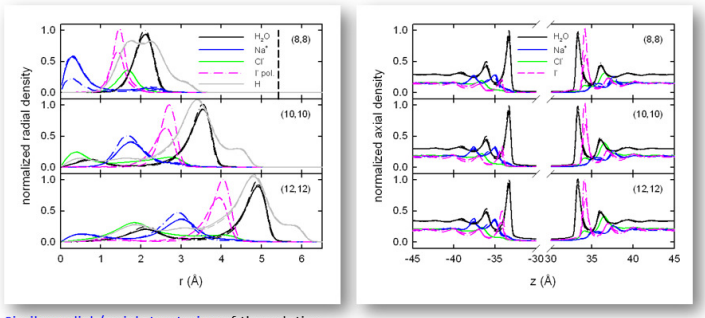

Similar radial / axial structuring of the solution.

I^- is optimally hydrated by the water boundary layer; polarizability enhances maxima.

Cl^- resides preferentially on the interior side of the Na^+ layer.

Carbon nanotubes for filtration/separation applications
Transport properties

Average number of ion passages
as a function of the pore radius

Average ion passage time
as function of the axial electric field

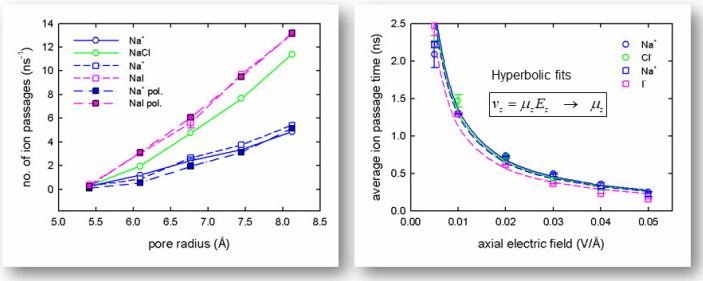

Net currents for NaI exceed those for NaCl by up to 30% – anion selectivity.

The I^- ions travel preferentially along cylindrical layers of larger radius than the Cl^- ions.

Partial Na^+ currents are solute independent.

Solvation dynamics of calcite
$CaCO_3$ unit cell – 1014 plane

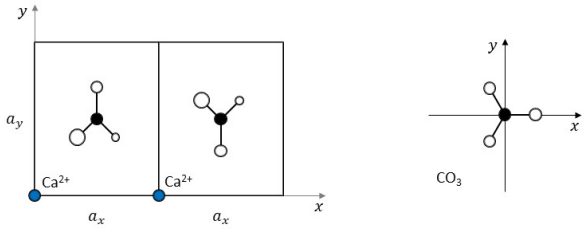

In-plane unit cell size
$a_x = 4.0485, \quad a_y = 4.991$

Inter-plane distance
$a_z = 3.036$

Inter-plane shift
$h_x = -0.76a_x, \quad h_y = -\frac{a_y}{2}$

Solvation dynamics of calcite
$CaCO_3$ unit cell – 1014 plane

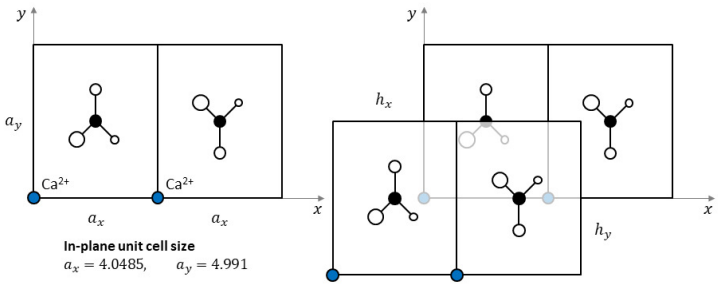

In-plane unit cell size

$a_x = 4.0485, \quad a_y = 4.991$

Inter-plane distance

$a_z = 3.036$

Inter-plane shift

$h_x = -0.76a_x, \quad h_y = -\frac{a_y}{2}$

Solvation dynamics of calcite

Slab model formed of 7 calcite ($CACO_3$) layers and 2 water reservoirs (side view)

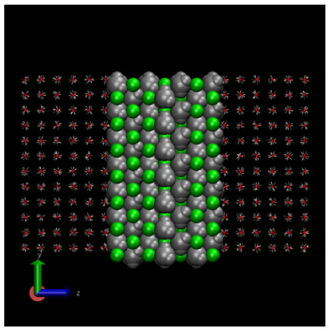

Slab model formed of 7 calcite ($CACO_3$) layers and 2 water reservoirs (top view)

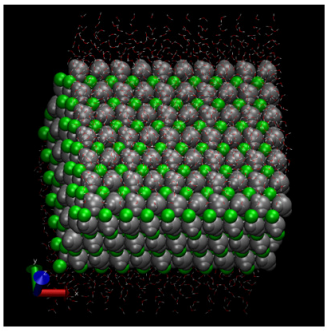

Solvation dynamics of calcite

Slab model formed of 7 calcite ($CACO_3$) layers with etch island

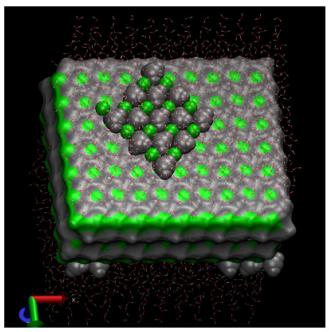

Slab model formed of 7 calcite ($CACO_3$) layers with etch pit

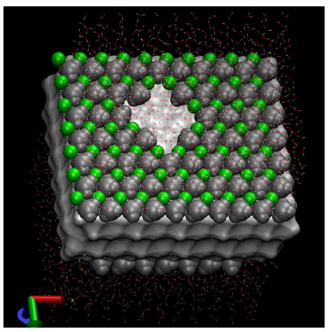

Solvation dynamics of calcite

Slab model formed of 7 calcite ($CACO_3$) layers with etch island

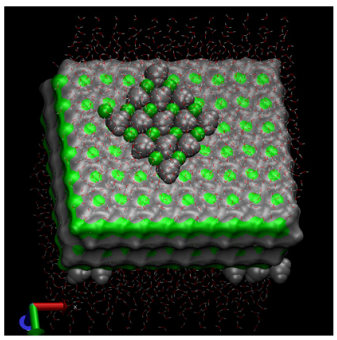

Solvation rates (blue – low, red – high)

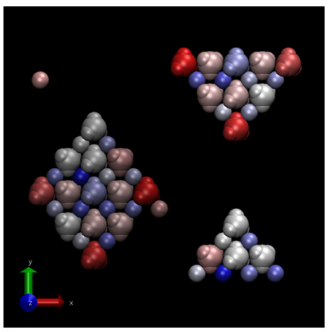

Solvation dynamics of calcite

Slab model formed of 7 calcite ($CACO_3$) layers with etch island

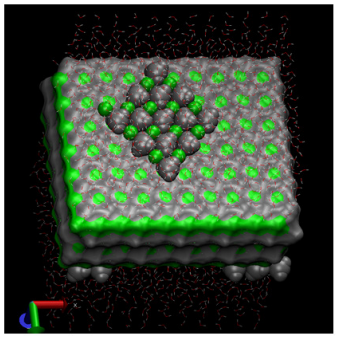

Solvation rates (blue – low, red – high)